

# Localization of the Kinesin Adaptor Proteins Trafficking Kinesin Proteins 1 and 2 in Primary Cultures of Hippocampal Pyramidal and Cortical Neurons

AQ1 **Omar Loss** and **F. Anne Stephenson\***

School of Pharmacy, University College London, London, United Kingdom

Neuronal function requires regulated anterograde and retrograde trafficking of mitochondria along microtubules by using the molecular motors kinesin and dynein. Previous work has established that trafficking kinesin protein (TRAK) 1 and TRAK2 are kinesin adaptor proteins that link mitochondria to kinesin motor proteins via an acceptor protein in the mitochondrial outer membrane, the Rho GTPase Miro. Recent studies have shown that TRAK1 preferentially controls mitochondrial transport in axons of hippocampal neurons by virtue of its binding to both kinesin and dynein motor proteins, whereas TRAK2 controls mitochondrial transport in dendrites resulting from its binding to dynein. This study further investigates the subcellular localization of TRAK1 and TRAK2 in primary cultures of hippocampal and cortical neurons by using both commercial antibodies and anti-TRAK1 and anti-TRAK2 antibodies raised in our own laboratory (in-house). Whereas TRAK1 was prevalently localized in axons of hippocampal and cortical neurons, TRAK2 was more prevalent in dendrites of hippocampal neurons. In cortical neurons, TRAK2 was equally distributed between axons and dendrites. Some qualitative differences were observed between commercial and in-house-generated antibody immunostaining. © 2015 Wiley Periodicals, Inc.

**Key words:** kinesin adaptor proteins; miro; mitochondrial transport; trafficking kinesin binding protein; TRAK

Twenty percent of the body's resting energy is consumed by the brain despite the brain being only 2% of the body's weight. This energy, in the form of ATP, is essential for correct neuronal function during synaptic and action potential signaling in neurons (Attwell and Laughlin, 2001). Because most brain ATP is generated by mitochondria, this implies that mitochondria must be spatially adjacent to the sites of the ion influxes that generate synaptic and action potentials. The main carbon source for ATP production by mitochondria is glucose. Proper neuronal metabolism is therefore dependent on a continuous supply of glucose (Peppiatt and Attwell, 2004). Mitochondria are actively mobile in neurons, and it was recently shown that mitochondrial dynamics are regulated

by glucose levels via the regulation of proteins associated with mitochondrial transport (Pekkurnaz et al., 2014).

At any given time, ~20–30% of the total mitochondria population is mobile (Pilling et al., 2006; Kang et al., 2008), so proper transport and targeting of mitochondria from the cell body (where they are concentrated) into dendrites and axons is essential for the function and support of synapses. Defective mitochondrial trafficking and function are increasingly implicated in neurological diseases (for review see Chan, 2006; Mattson et al., 2008).

In both axons and dendrites, the majority of mitochondrial transport is microtubule based. Mitochondria undergo alternating outward (anterograde) and inward (retrograde) transport. Their movement from neuronal cell bodies into axonal and dendritic synaptic terminals is regulated by a quaternary mitochondrial trafficking complex. This is composed of the motor proteins kinesin or dynein, the trafficking kinesin protein (TRAK) family of kinesin adaptor proteins, the TRAK acceptor, the mitochondrial outer membrane Rho GTPase Miro, and the posttranslational modification enzyme N-acetylglucosamine transferase (OGT; for review see Stephenson and Brickley, 2011; Schwarz, 2013).

In mammals, there are two members of the TRAK family, TRAK1 and TRAK2, whereas *Drosophila* has only one TRAK gene, named *Milton*. TRAK1 and TRAK2 share an overall 48% amino acid identity and a 58% amino acid sequence similarity (Beck et al., 2002; Iyer et al., 2003). Both TRAK1 and TRAK2 are known to interact with Miro (Glater et al., 2006).

Recently, it was reported that TRAK1 binds to both kinesin and dynein motor proteins and that it is

Contract grant sponsor: BBSRC; Contract grant number: BB/K014285/1

\*Correspondence to: Prof. F. Anne Stephenson, School of Pharmacy, University College London, 29/39 Brunswick Square, London WC1N 1AX, United Kingdom. E-mail: anne.stephenson@ucl.ac.uk

Received 7 October 2014; Revised 28 November 2014; Accepted 2 December 2014

Published online 00 Month 2015 in Wiley Online Library (wileyonlinelibrary.com). DOI: 10.1002/jnr.23549

## 2 Loss and Stephenson

localized primarily in axons of hippocampal pyramidal neurons in primary culture. In contrast, TRAK2 was shown to interact predominantly with dynein, and it is more abundant in dendrites compared with axons (van Spronsen et al., 2013). These findings reflect those of previous studies in which trafficking assays in hippocampal neurons were employed to show that kinesin motors specifically target axons and drive synaptic vesicle transport, whereas the dynein/dynactin motor complex sorts postsynaptic receptors and Golgi outposts to dendrites (Zheng et al., 2008; Kapitein et al., 2010). This study investigates further the purported compartmentalization of TRAK1 and TRAK2, extending studies to their respective distributions in both hippocampal and cortical primary cultures by using both commercial antibodies and anti-TRAK1 and anti-TRAK2 antibodies raised in our own laboratory (in-house).

### MATERIALS AND METHODS

#### Constructs and Antibodies

The plasmids pEGFP-ratTRAK1 (pEGFP-rTRAK1), pCis-rTRAK2, pDsRedTRAK1scrRNA, pDsRedTRAK1shRNA, pGreenTRAK2scrRNA, and pGreenTRAK2shRNA were as described previously by Brickley and Stephenson (2011). Rabbit polyclonal anti-TRAK1 antibodies were generated to the amino acid sequence Cys rat TRAK1 (973–988) and affinity-purified by following standard protocols (Stephenson and Duggan, 1991). Sheep anti-TRAK2 (874–889) antibodies were generated as described by Brickley et al. (2005). Anti-TRAK1 (catalog No. HPA005853), anti-TRAK2 (catalog No. HPA015827), and anti- $\beta$ -actin commercial antibodies were purchased from Sigma Aldrich (Dorset, United Kingdom). Mouse monoclonal anti-tau (tau-5) and antimicrotubule associated protein 2 (MAP2; HM-2) antibodies were purchased from Abcam (Cambridge, United Kingdom). Goat anti-rabbit Alexa Fluor 594 and 488, goat anti-sheep Alexa Fluor 594 and 488, and goat anti-mouse Alexa Fluor 594 secondary antibodies were from Life Technologies (Paisley, Scotland).

#### Mammalian Cell Transfections

Human embryonic kidney (HEK) 293 cells were transfected with constructs by the calcium phosphate method by using 1  $\mu$ g total DNA/six-well plate. For double transfections, a 1:1 ratio for a total of 2  $\mu$ g DNA was used/six-well plate. Cells were harvested 48 hr posttransfection and solubilized with standard radioimmunoprecipitation assay buffer (1% [v/v] Triton X-100, 0.5% [w/v] Na-deoxycholate, 0.1% [w/v] SDS, 150 mM NaCl, 1 mM EDTA, 10 mM NaF, 1 mM PMSF, 0.5  $\mu$ g/ml protease inhibitor cocktail). For confocal studies, HEK 293 cells were transfected with constructs by the Lipofectamine 2000 (Life Technologies) method with 0.5  $\mu$ g total DNA/24-well plate. For double transfections, a 1:1 ratio for a total of 1  $\mu$ g DNA was used/24-well plate.

#### Immunoblotting

Immunoblotting was carried out exactly as described by Brickley et al. (2005) by using final antibody concentrations of

1  $\mu$ g/ml anti-TRAK1 (973–988), 2  $\mu$ g/ml anti-TRAK2 (874–889), 0.2  $\mu$ g/ml commercial anti-TRAK1, and 0.4  $\mu$ g/ml commercial anti-TRAK2.

#### Culturing and Transfection of Hippocampal and Cortical Neurons

Cultures of rat hippocampal and cortical neurons were prepared at a density of  $\sim$ 30,000 cells/cm<sup>2</sup> on poly-D-lysine (1  $\mu$ g/ml)- and laminin (2  $\mu$ g/ml)-coated coverslips from hippocampi or cerebral cortex dissected from E18 rat embryos by standard methods (Goslin et al., 1998). Cultures were grown for 4–8 days in complete neurobasal media that consisted of neurobasal media (Life Technologies) containing a 1:50 dilution of B27 (Life Technologies), 0.5 mM GlutaMax (Life Technologies), 0.4% (w/v) glucose, and 1 $\times$  penicillin/streptomycin. Transfection of neurons was by Lipofectamine LTX (Life Technologies). In brief, 24 hr prior to transfection, complete neurobasal medium with antibiotics was replaced by fresh complete neurobasal medium without antibiotics. Subsequently, one-half of the medium was removed and stored at 37°C in 5% CO<sub>2</sub>. The transfection reaction was performed according to the manufacturer's protocol. For all transfections, 0.5  $\mu$ g EndoFree plasmid DNA was added per 24-well dish. After addition of the transfection mixture, neurons were incubated at 37°C in 5% CO<sub>2</sub>, and the previously removed medium was then added. Neurons were maintained at 37°C in the presence of 5% CO<sub>2</sub> until paraformaldehyde fixation (48–72 hr). For the short hairpin RNAi (shRNAi) knockdown studies, neuronal transfections were carried out at 3–4 days in vitro (DIV), with paraformaldehyde fixation at 6–7 DIV.

#### Immunocytochemistry

Fixed cells (6–7 DIV) were permeabilized and blocked with a solution containing 0.2% (v/v) Triton X-100 (Sigma) and 10% (v/v) fetal bovine serum in phosphate-buffered saline (PBS) for 1 hr at room temperature. Primary antibodies were diluted in the solution to final concentrations of 10  $\mu$ g/ml anti-TRAK1 (973–988), 20  $\mu$ g/ml anti-TRAK2 (874–889), 0.5  $\mu$ g/ml commercial anti-TRAK1, and 1.0  $\mu$ g/ml commercial anti-TRAK2, then added to the cells and incubated overnight at 4°C. Cells were washed three times with PBS (137 mM NaCl, 2.7 mM KCl, 10 mM Na<sub>2</sub>HPO<sub>4</sub>, 1.8 mM KH<sub>2</sub>PO<sub>4</sub>, pH 7.4) containing 0.1% (v/v) Tween 20 (Sigma) for 10 min with gentle rotation. Secondary antibodies were added at a dilution five times the concentration of the corresponding primary antibodies and incubated for 1 hr at room temperature. Coverslips were washed three times with PBS containing 0.1% (v/v) Tween 20 for 10 min with gentle rotation prior to fixation with 2% (w/v) paraformaldehyde for 5 min at room temperature. After having been washed an additional three times in PBS, coverslips were mounted onto microscopy slides with 10  $\mu$ l fluorescence mounting solution (Dako, Agilent Technologies, Stockport, United Kingdom). Nuclei were visualized by staining with 4',6-diamidino-2-phenylindole (DAPI).

#### Confocal Microscopy and Image Analysis

Confocal microscopy was carried out with a Zeiss LSM 710 (Carl Zeiss, Oberkochen, Germany) confocal microscope

with oil immersion  $\times 40$  or  $\times 63$  objectives with sequential acquisition setting. EGFP was excited with  $\lambda = 488$  nm at 2% of intensity. Alexa Fluor 594 was excited with  $\lambda = 561$  nm at 2% intensity. Z-stacks of cells and neurons were taken at a resolution of  $1024 \times 1024$  pixels with the pinhole at a setting of  $2 \mu\text{m}$  in the Zen Lite Blue software (Carl Zeiss), ensuring that image saturation was not reached. Maximum projection intensities were generated, and images were analyzed in ImageJ (NIH). All cells and neurons were imaged as z-stacks, and maximum projection intensities were generated for image presentation. All experiments were from at least  $n = 20$  neurons from at least  $n = 3$  cultured neuronal preparations.

For the analysis of antibody intensities in neurons, tau/MAP2 counterstaining was used to distinguish between axons and dendrites. Fluorophore intensities were determined in the ImageJ plugin RGB profile (RGB\_Profiler.java). To prevent selection bias, cell bodies, axons, and dendritic segments were selected in the red channel (tau or MAP2 immunoreactivities) and quantified in the green channel (TRAK1 and TRAK2 immunoreactivities). The fluorescence intensities in axons and dendrites were measured in segments of the same size and normalized to the intensity of the cell bodies. To control for background fluorescence, the intensity adjacent to the axon or dendrite was subtracted.

## RESULTS

### Comparison of the Epitopes Used To Generate Anti-TRAK1 and Anti-TRAK2 Antibodies

In any microscopy/immunocytochemical study, the specificity of the antibodies used is key, especially when members of the same family of proteins share high percentages of amino acid identities. This is the case for TRAK1 and TRAK2, which have 48% identity (Beck et al., 2002). Thus, the immunogens that have been used to generate anti-TRAK1 and anti-TRAK2 antibodies were compared. These included TRAK1 and TRAK2 in-house antibodies, commercial antibodies, and those used previously by van Spronsen et al. (2013) to study the distribution of TRAK1 and TRAK2 in primary neurons. The comparison of the immunogens is shown in Figure

F1 1.

For the commercial anti-TRAK1 and anti-TRAK2 antibodies, the antigens used for their generation were fusion proteins corresponding to TRAK1 (238–470) and TRAK2 (359–488). These regions share  $\sim 37\%$  amino acid identity and  $\sim 58\%$  similarity and contain three stretches of five, five, and 12 contiguous amino acid sequences that are identical between TRAK1 and TRAK2 (Fig. 1B). Similarly, fusion proteins were used for the generation of anti-TRAK1 and anti-TRAK2 antibodies by van Spronsen et al. (2013). The chosen sequences were from the TRAK1 and TRAK2 C-termini, i.e., TRAK1 (754–953) and TRAK2 (848–913). The C-terminal domain is the least conserved region between TRAK1 and TRAK2, but regions of amino acid identity are still evident (Fig. 1B). Indeed, these fusion proteins share 31% amino acid identity and  $\sim 68\%$  similarity. In contrast, in-house antibodies were generated by using

short synthetic peptides corresponding to the nonconserved C-terminal regions, i.e., TRAK1 (973–988) and TRAK2 (874–889). Within these sequences, amino acid identity is 33% and similarity is 69% but with a maximum of two contiguous identical amino acids (Fig. 1B).

### Characterization of Anti-TRAK1 and Anti-TRAK2 Antibodies

To assess the specificity of the various anti-TRAK1 and anti-TRAK2 antibodies, an shRNA gene knock-down approach was used, followed by analysis of samples by immunoblotting and immunocytochemistry.

**Immunoblotting.** HEK 293 cells were cotransfected with pEGFP-rTRAK1 or pCis-rTRAK2 and either the shRNA constructs pDsRedTRAK1shRNA and pGreenTRAK2shRNA or the corresponding control scrambled scr constructs, i.e., pDsRedTRAK1scrRNA or pGreenTRAK2scrRNA (Brickley and Stephenson, 2011). For Western blot analyses, cell lysates were produced 48–72 hr posttransfection and analyzed with their antibodies. (Note that HEK 293 cells do not express endogenous TRAK1 and TRAK2 [Beck et al., 2002].)

In HEK 293 cells cotransfected with pEGFP-rTRAK1 and either the scrRNA or the shRNA constructs, in-house anti-TRAK1 antibodies recognized a major band with  $M_r \sim 120$  kDa, which corresponds to the predicted molecular weight of pEGFP-rTRAK1 (Fig. 2A). This  $M_r \sim 120$ -kDa band was not detectable in cells cotransfected with pCis-rTRAK2 and the scrRNA or shRNA constructs, although a nonspecific band with  $M_r \sim 70$  kDa was observed in all samples. HEK 293 cell lysates cotransfected with pEGFP-rTRAK1 and pDsRed-TRAK1shRNA showed a  $47\% \pm 16\%$  ( $n = 3$ ) reduction in the  $M_r$  120-kDa immunoreactive band with no observed qualitative change in the  $M_r \sim 70$ -kDa nonspecific band (Fig. 2A). Similarly, anti-TRAK1 commercial antibodies recognized TRAK1, i.e.,  $M_r$  120 kDa, in the HEK 293 cell lysates, and this was decreased by  $66\% \pm 9\%$  ( $n = 3$ ) in the presence of TRAK1 shRNA. However, they also recognized a band that corresponds to the predicted size of pCis-rTRAK2, i.e.,  $M_r$  98 kDa, in samples that were transfected with pCis-rTRAK2 and the TRAK2 scrRNA or shRNAs. The percentage reduction in signal for the  $M_r$  98-kDa TRAK2 species was  $38\% \pm 7\%$  ( $n = 3$ ).

F2

In HEK 293 cells cotransfected with pEGFP-rTRAK2 and either the scrRNA or the shRNA constructs, in-house anti-TRAK2 antibodies recognized a single band with  $M_r \sim 98$  kDa, which corresponds to the predicted molecular weight of pCisTRAK2 (Fig. 2A). A second minor band at  $M_r$  110 kDa was also detected. No band was visible in HEK 293 cells cotransfected with pEGFP-rTRAK1 and corresponding shRNAs. The  $M_r$  98-kDa band had an observed  $29\% \pm 8\%$  ( $n = 3$ ) reduction when immunoblots from pDsRedTRAK2shRNA vs. pGreenTRAK2scrRNA cotransfectants were compared (Fig. 2A). Similarly, commercial anti-TRAK2 antibodies recognized TRAK2 with  $M_r \sim 98$  kDa in the

4 Loss and Stephenson

**A**  
**Human-TRAK1**

```
MALVFQFGQPVRAQLPGLCHGLRTNACDVCNSTDLPEVEIISLLEEQLPHYKLRADTIYGYDHDHWLHTPLISPDANIDLTE
QIEETLKYFLLCAERVGQMTKYNDIDAVTRLLEEKERDLELAARIGQSLKKNKTLTERNELLEEQVEHIREEVSQLRHELMSMKD
ELLQFYTSAAEESEPEVCSVCTPLKRNESSSVQNYFHLDLSLQKLDLEENNVLRSEASQLKTEITITYEKEQQLVNDCKELR
DANVQIASISEELAKKTEDAARQEEITHLLSQIVDLQKKAKACAVENEELVQHLGAAKDAQRLTAELFELEDKYAECMEMLHE
AQEELKNLRNKTMPNNTSRRYHSLGLFPMDSLAAEIEGTMRKELQLEAEASPDITHQKRVFETVRNINQVVKQRSLTPSPMNI
SNQSSAMNSLLSSCVSTPRSSFYGSIDIGNVVDNKTNSIILETEAADLGNDRSKKPGTPTGPGSHDLETALRRLSLRRENYLSE
RRFFEEERKRLQELAEKELRSGSLTPTESIMSLGTHSRFSEFTGFGSGMSFSSRSYLPKQLQIVKPLEGSATLHHWQQLAQPH
LGGILDPRPGVVTGFRFLDVLDEYCLNDFEEDDGDHISLPRLATSTPVQHPETSAHHPGKCMSQTNSTFTTTCRILHPSD
ELTRVYPSLNSAPTPACGSTSHLKSTPVATPCTPRRLSLAESFTNTRESTTTMSTSLGLVWLLKERGISAAVYDPQSWDRAGRG
SLLHSYTPKMAVIPSTPPNSPMQPTPTSSPPSFEFKCTSPPYDNFLASKPASSILREVREKNRVSSESQTDVSVSNLNLVDKVRRF
GVAKVVNSGRAHVPTLTEEQGPLCGPPGAPALVPRGLVPEGLPRLCPTVTSAIGGLQLNSGIRNRNSFPTMVGSSMQMKAP
VTLTSGILMGAKLSKQTSLR
```

Commercial  
In House  
Van Spronsen et al.

**Human-TRAK2**

```
MSQSQNAIFTSPTGEENLMNSNHRDSEITDVCNSNEDLPEVELVSLLEEQLPQYRLKVDTLFLYENQDWTQSPHQRHASDALS
PVLAEETFRYMILGDRVEQMTKYNDIDIMVTHLLAERDRDLAARIGQALLKRNHVLSEQNESLEEQLGQAFDQVNLQHEL
CKKDELLRIVSIAESEETDSSCSTPLRFNESFSLSQGLLQLEMLQEKLEEEENMALRSKACHIKTETVYEEKEQQLVSDCVK
ELRETNQMSRMTEELSGKSDLELIRYQEEELSSLSQIVDLQHLKEHVIEKEELKLHLQASKDAQRLTMELHELQDRNMECLG
MLHESQEEIKELRSRSGPTAHLYFSQSYGAFTGESLAAEIEGTMRKLSLDEESSLFKQKQKRVFDTVRIANDTRGRSISFPA
LLPIPGSNRSSVIMTAKPFESGLQQTEDKSLLNQGSSEEVAGSSQKMGQPGSGSDLATALHRLSLRRQNYLSEKQFFAAE
WQRKIQVLADQKEGVSGCVPTTESLASLCTTQSEITDLSASCLRGFMPEKLQIVKPLEGSATLHHWQQLAQPNLGTLDPRPG
VITKGTQLPGDAIYHISDLEEEDEEGITFVQVQPLEVEEKLSTSKPVTGIFLPPITSAGGPVTATANPGKCLSCNSTFTTTCRI
LHPSDITQVTPSSGFPPLSCGSSGSSSNTAVNSPALSYRLSIGESITNRRDSTTTFSSTMSLAKLLQERGISAKVYHSPISENPLQ
PLPKSLAIPSTPPNSPSPHPCPSPLPFEPVHLSENFLASRPAETFLDEMYGLRPSRNPPDVGQKMNLDRLKRLGIARVVKNP
GAQENGRQCEAEIGPKPDSAVYNSGSSLLGGLRRNQSFPVIMGSFAAPVCTSSPKMGVLKED
```

Commercial  
In House  
Van Spronsen et al.

**B**

**Commercial**

TRAK1	ELEDKYAECMEMLHEAQEELKNLRNKTMPNNTSRRYHSLGLFPMDSLAAEIEGTMRKELQ	60
TRAK2	-----HLYFSQSYGAFTGESLAAEIEGTMRKCLS	29
	: * * * : ***** : *	
TRAK1	LAEAES--PDITHQKRVFETVRNINQVVKQRSLTPSPMNI PGSNQSSAMN-----	108
TRAK2	LDSEESLQKQKQKRVFDTVRIANDTRGRSISFPALLPIPGSNRSSVIMTAKPFESGLQ	89
	* : * * : : ***** : * : * : * : * : * : *	
TRAK1	-----SLLSSCVSTPRSSFYGSIDIGNVVDNKTNSIILET-	143
TRAK2	QTEDKSLLNQGSSEEVAGSSQKMGQPGSGSDLATALHR	130
	*** * : : * : * : * : *	

**In House**

TRAK1	---SGILMGAKLPKQTSLR	16
TRAK2	CNSGGSLGG-LRRNQL-	17
	. * * : * : *	

**Van Spronsen et al.**

TRAK1	YDPQSWDRAGRGSLLHSYTPKMAVIPSTPPNSPMQPTPTSSPPSFEFKCTSPPYDNFLASK	60
TRAK2	-----	
TRAK1	PASSILREVREKNRVSSESQTDVSVSNLNLVDKVRRFVAKVVNSGRAHVPTLTEEQGPL	120
TRAK2	-----EMYGLRPSRNPPDVGQKMNLDRLKRLGIARVVKNP GAQENGRQCEA---	48
	. : * * . . * * : : * * : : * * : : * * : * : *	
TRAK1	LCGPPGAPALVPRGLVPEGLPRLCPTVTSAIGGLQLNSGIRNRNSFPTMVGSSMQMKAP	180
TRAK2	EIGPQKPDASAVLN-----SGSLLGGLRRNQSFPVIMGSFAAPVCT	90
	** * * : . * * * * : * * * * : * * * * : *	
TRAK1	VTLTSGILMGAKLSKQTSLR	200
TRAK2	SSPKMGVLKE-----	100
	. * * *	

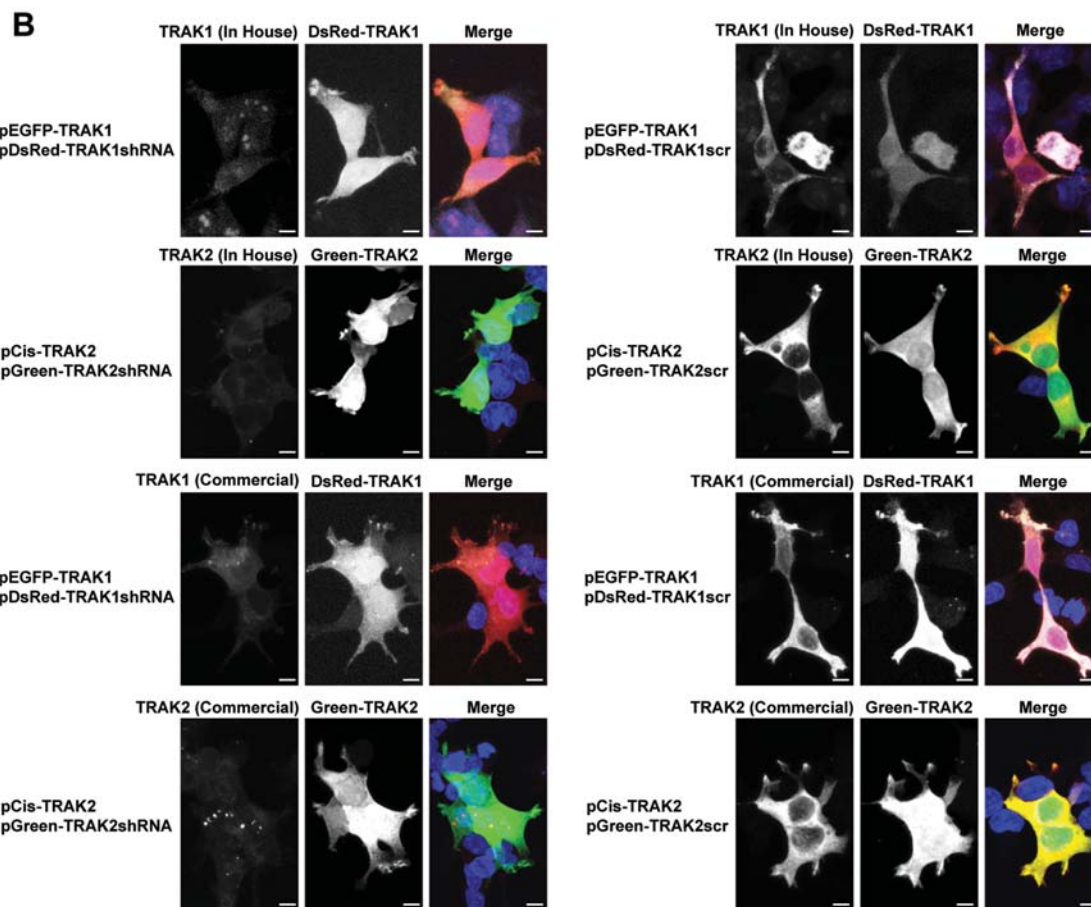
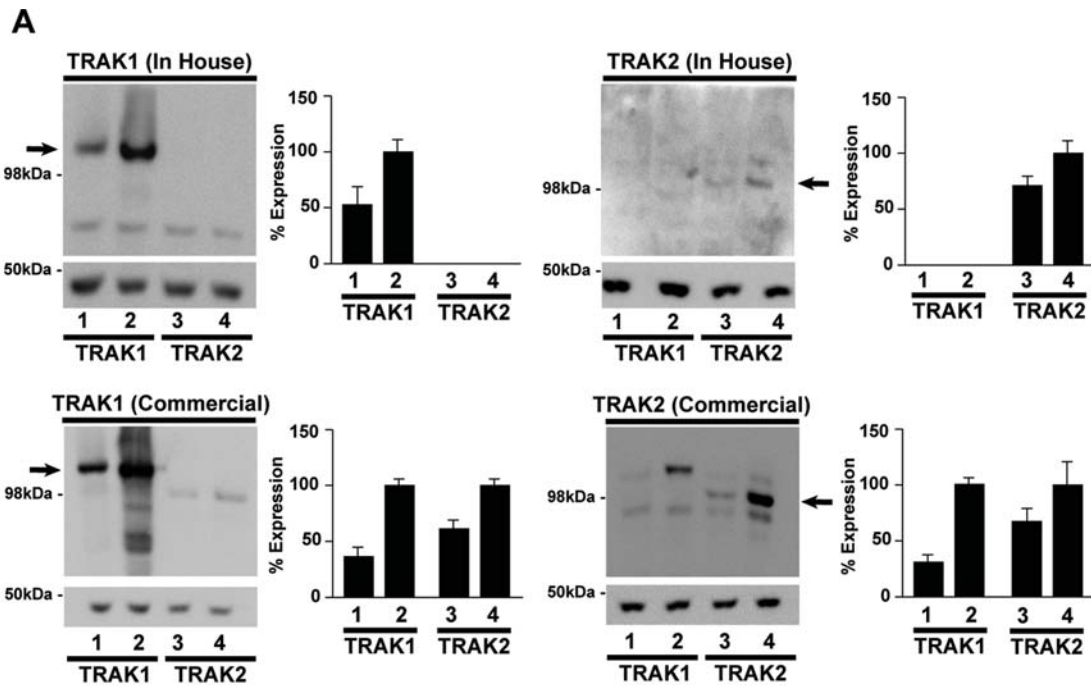
Fig. 1. Comparison of the amino acid sequences used to generate anti-TRAK1 and anti-TRAK2 antibodies. **A:** Amino acid sequences of human TRAK1 and human TRAK2 with the amino acid sequences of the immunogens used for the generation of anti-TRAK1 (top) and anti-TRAK2 (bottom) shown in the rectangles. Note that, for the

in-house anti-TRAK1 antibodies, a rat TRAK1 sequence was used, but the equivalent aligned human TRAK1 sequence is shown. **B:** Clustal Omega alignment of the immunogens used for the generation of anti-TRAK1 and anti-TRAK2 antibodies. For in-house rTRAK1 antibodies, it is the rat sequence that is shown.

Localization of TRAK1 and TRAK2 5

HEK 293 cells. A 32% ± 13% (n = 3) decrease in this band was detected in cells transfected with pCis-rTRAK2 and pGreenTRAK2shRNA compared with those trans-

fected with the pGreenTRAK2scrRNA control (Fig. 2A). However, as for the commercial anti-TRAK1 antibodies, anti-TRAK2 antibodies also recognized a band



COLOR

6 Loss and Stephenson

corresponding to the molecular size of pEGFP-rTRAK1, i.e.,  $M_r \sim 120$  kDa, in HEK 293 cells transfected with pEGFP-rTRAK1. The percentage reduction in signal for the  $M_r$  98-kDa TRAK2 species was  $75\% \pm 6\%$  ( $n = 3$ ). A second band at  $M_r \sim 85$  kDa was also detected by commercial anti-TRAK2 antibodies in the samples cotransfected with both the TRAK1 and the TRAK2 constructs and either the scrRNA or the shRNA. Table I summarizes the specificities of the anti-TRAK1 and anti-TRAK2 antibodies.

**Immunocytochemical analyses of HEK 293-transfected cells.** For the immunocytochemical studies, HEK 293 cells were fixed 48–72 hr posttransfection, and immunostaining was performed with in-house and commercial anti-TRAK1 and anti-TRAK2 antibodies. Cells cotransfected with pEGFP-rTRAK1 and pDsRed-TRAK1scrRNA stained with in-house anti-TRAK1 antibodies coupled with anti-rabbit Alexa Fluor 680 revealed immunostaining in HEK 293 cell bodies and a higher expression in the perinuclear region and at the tip of cellular processes, as previously described for both TRAK1 and GFP-tagged TRAK1 (Fig. 2B; Brickley et al., 2005, 2011). No fluorescence was evident in HEK 293 cells cotransfected with pEGFP-rTRAK1 and pDsRedTRAK1shRNA and stained with in-house anti-TRAK1 antibodies. Similar results were obtained with regard to both distribution and specificity for commercial anti-TRAK1 antibodies (Fig. 2B).

HEK 293 cells cotransfected with pCis-rTRAK2 and pGreenTRAK2scrRNA stained with in-house anti-

TRAK2 antibodies coupled with anti-rabbit Alexa Fluor 594 revealed similar patterns of fluorescence, as they did for labeling with anti-TRAK1 antibodies; i.e., localization was evident in cell bodies, but higher expression was detected in the perinuclear region and at the tip of cellular processes, again, as previously described for TRAK2 and GFP-TRAK2 (Brickley et al., 2005, 2011). No fluorescence was evident in HEK 293 cells cotransfected with pEGFP-rTRAK1 and pDsRedTRAK1shRNA and stained with in house anti-TRAK2 antibodies (Fig. 2B). Table I summarizes the specificities of the anti-TRAK1 and anti-TRAK2 antibodies.

**Immunocytochemical analyses of endogenous TRAK1 and TRAK2 in primary neuronal cultures.** To determine the specificity of the in-house and commercial anti-TRAK antibodies in primary neuronal cultures, 4-DIV hippocampal and 4-DIV cortical neurons were transfected with pDsRedTRAK1shRNA, pGreenTRAK2shRNA, or the corresponding scrambled control shRNAs, i.e., pDsRedTRAK1scrRNA or pGreenTRAK2scrRNA. Neurons were fixed 48–72 hr posttransfection, and immunostaining was performed as described in Materials and Methods.

All anti-TRAK1 and anti-TRAK2 antibodies showed immunofluorescent staining in both primary hippocampal (Fig. 3) and cortical (Fig. 4) neurons. Both in-house and commercial antibodies showed similar profiles for immunostaining for TRAK1 in cortical and hippocampal neurons and, similarly, for TRAK2 in cortical and hippocampal neurons. Anti-TRAK1 immunoreactivity was strongest in the perinuclear region. It was also distributed throughout the neurons, including axonal and dendritic processes. Anti-TRAK2 immunoreactivity was also enriched in the perinuclear region, and, in addition, it was distributed in the cytoplasm and dendritic and axonal processes, although the labeling of processes was less clear than was found for labeling with anti-TRAK1 antibodies. It is noteworthy that an accumulation of both TRAK1 and TRAK2 immunoreactivities was noticed at the tips of differentiating axons. This most likely coincides with the growth cone of the axons.

Transfection of pDsRedTRAK1scrRNA or pGreenTRAK2scrRNA had no effect on the expression of TRAK1 or TRAK2 in both hippocampal and cortical neurons. This can be seen in Figures 3 and 4, in which

**TABLE I. Summary of the Specificities of the Commercial and In-House Anti-TRAK1 and Anti-TRAK2 Antibodies\***

Antibody	Immunoblot		Immunofluorescence	
	TRAK1	TRAK2	TRAK1	TRAK2
TRAK1 in house	+++		+++	
TRAK2 in house		++		+++
TRAK1 commercial	++	+	++	+
TRAK2 commercial	+	++	+	+++

\*+ Indicates the relative specificity of the antibody, where +++ represents the highest specificity. For the immunofluorescence, the plus signs correspond to immunofluorescent staining of HEK 293 cells expressing either TRAK1 or TRAK2 (results not shown).

Fig. 2. Characterization of anti-TRAK1 and anti-TRAK2 in-house and commercial antibodies by Western blotting and immunocytochemistry. **A:** HEK 293 cells were cotransfected with pEGFP-rTRAK1 + pDsRedTRAK1shRNA (1), pEGFP-rTRAK1 + pDsRedTRAK1scrRNA (2), pCis-rTRAK2 + pGreenTRAK2shRNA (3), or pCis-rTRAK2 + pGreenTRAK2scrRNA (4) cell lysates prepared 24 hr posttransfection and analyzed by immunoblotting with in-house or commercial anti-TRAK1, anti-TRAK2, or anti- $\beta$ -actin antibodies as shown as described in Materials and Methods. Arrows indicate the positions of TRAK1 and TRAK2. Histograms show the percentage expression of exogenous TRAK1 or TRAK2 with respect to the scrRNA controls and are mean  $\pm$  SEM for  $n = 3$  independent transfection experiments. **B:** HEK 293 cells were cotransfected with

pEGFP-rTRAK1 + pDsRedTRAK1shRNA, pEGFP-rTRAK1 + pDsRedTRAK1scrRNA, pCis-rTRAK2 + pGreenTRAK2shRNA, or pCis-rTRAK2 + pGreenTRAK2scrRNA and stained with the corresponding anti-TRAK1 or anti-TRAK2 in-house or commercial antibodies labeled as described in Materials and Methods. For all sets of images, the image at left shows transfected cells stained with the in-house and commercial anti-TRAK1 or anti-TRAK2 antibodies, the center image shows the fluorescence of the transfected shRNA or scrRNA constructs, and the image at right is the merged image for each panel. Blue is DAPI nuclear staining. Images are representative of at least  $n = 20$  cells from at least  $n = 3$  independent transfections. Scale bars = 10  $\mu$ m.

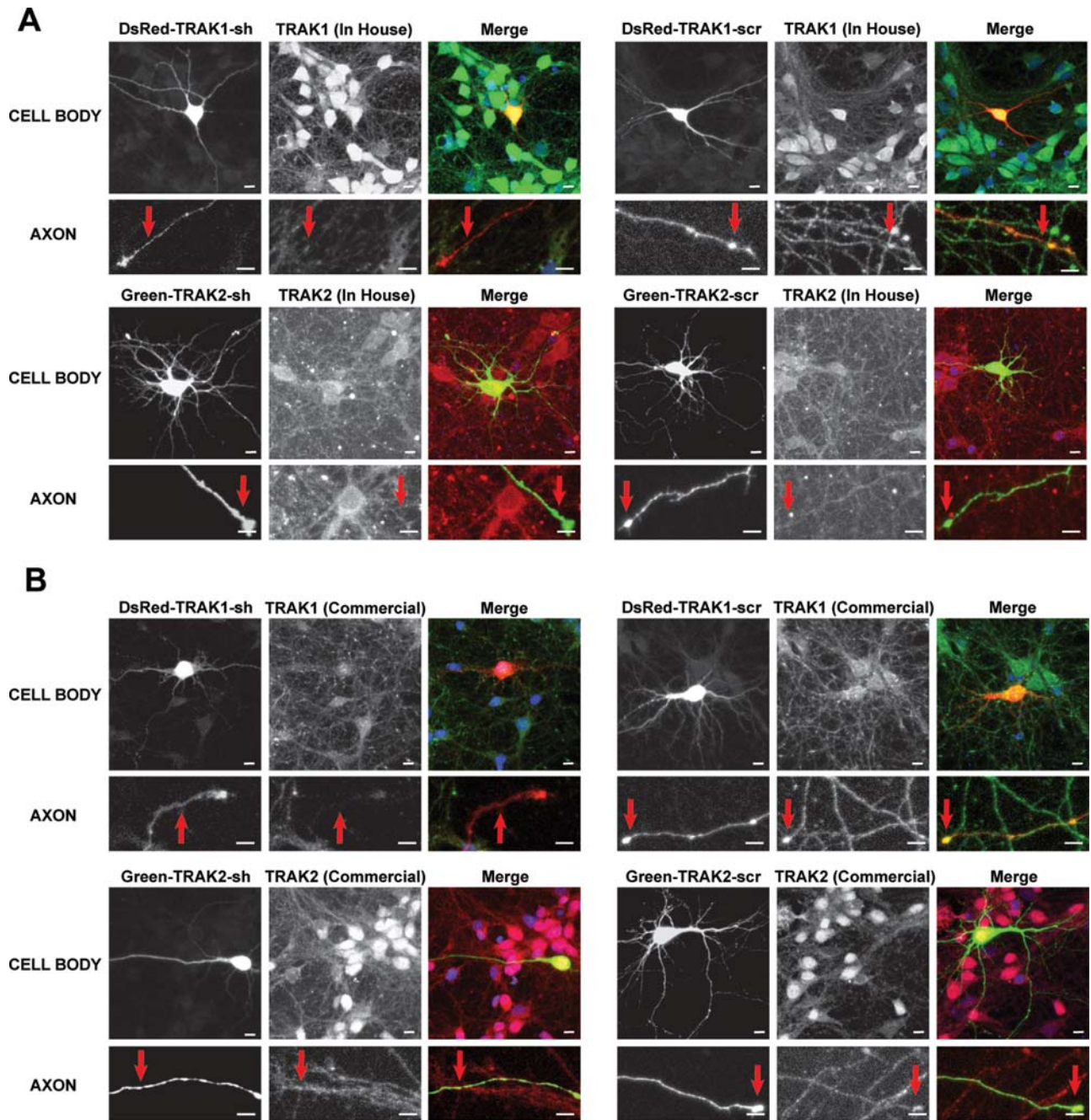


Fig. 3. Immunostaining of hippocampal pyramidal neurons with in-house and commercial anti-TRAK1 or anti-TRAK2 antibodies following gene knockdown with shRNAs. Primary cultures of hippocampal pyramidal neurons were transfected with pDsRedTRAK1shRNA, pDsRedTRAK1scrRNA, pGreenTRAK2shRNA, or pGreenTRAK2scrRNA at 3–4 DIV and stained with the corresponding in-house (A) or commercial (B) anti-TRAK1 and anti-TRAK2 antibodies at 6–7 DIV as described in Materials and Methods. In all cases, the image at left shows the fluorescence of the transfected shRNA or scrRNA constructs, the center image shows staining with

in-house (A) or commercial (B) anti-TRAK1 or anti-TRAK2 antibodies as labeled, and the image at right shows the merged image for each. Blue is DAPI nuclear staining. Top panels show cell bodies and bottom panels show selected axons; arrows highlight regions of pGreen- or DsRed-positive axons where TRAK1 and TRAK2 expression can be compared between shRNA and scrRNA in transfected vs. nontransfected neurons. Images are representative of at least  $n = 20$  hippocampal pyramidal neurons from at least  $n = 3$  independent transfections. Scale bars = 10  $\mu\text{m}$ .

COLOR

8 Loss and Stephenson

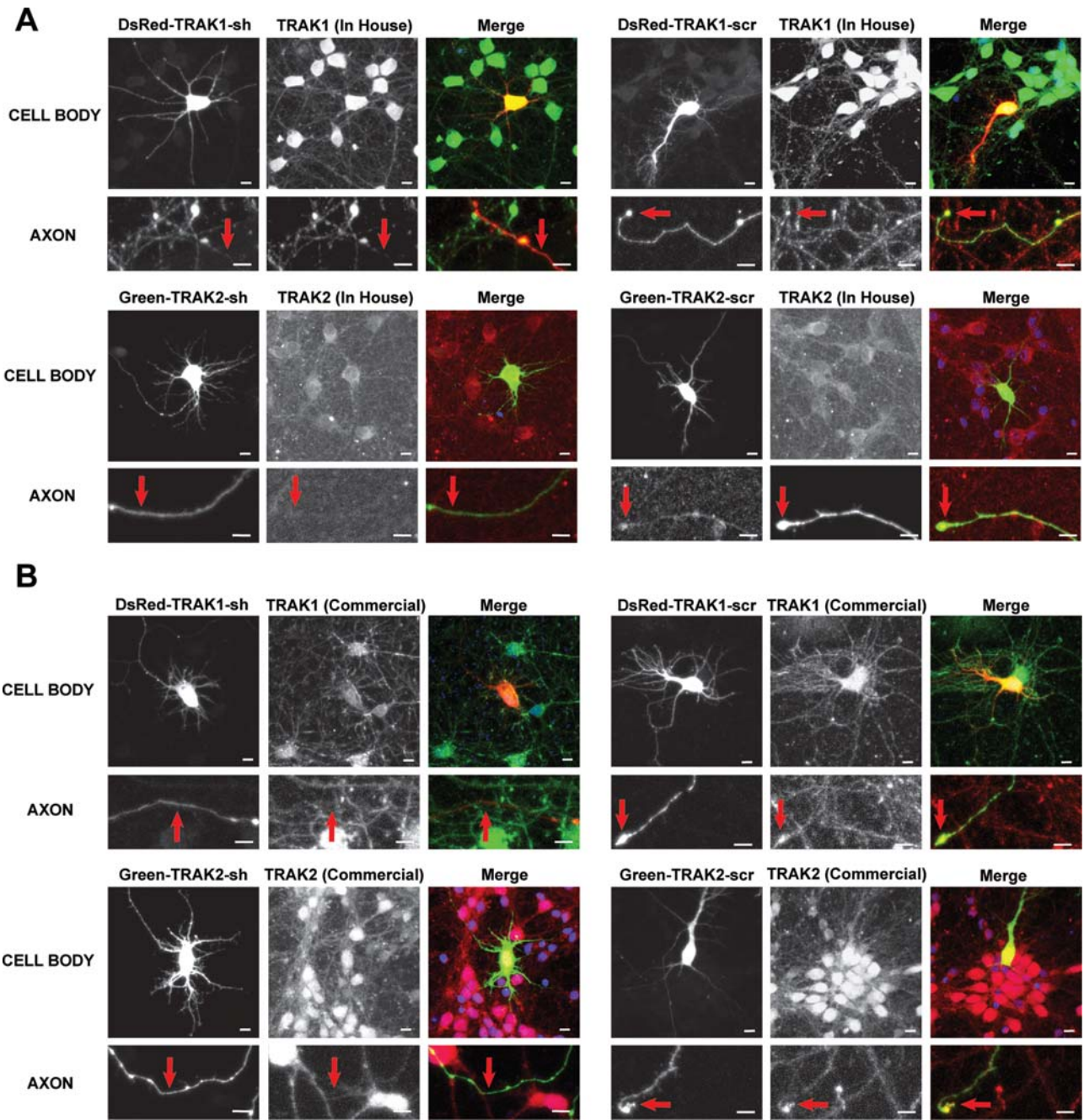


Fig. 4. Immunostaining of cortical neurons with in-house and commercial anti-TRAK1 and anti-TRAK2 antibodies following gene knockdown with shRNAs. Primary cultures of cortical neurons were transfected with pDsRedTRAK1shRNA, pDsRedTRAK1scrRNA, pGreenTRAK2shRNA, or pGreenTRAK2scrRNA at 3–4 DIV and stained with the corresponding in-house (A) or commercial (B) anti-TRAK1 and anti-TRAK2 antibodies at 6–7 DIV as described in Materials and Methods. In all cases, the image at left shows the fluorescence of the transfected shRNA or scrRNA constructs, the center

image shows staining with in-house (A) or commercial (B) anti-TRAK1 or anti-TRAK2 antibodies as labeled, and the image at right is the merged image for each. Blue is DAPI nuclear staining. Top panels show cell bodies, and the bottom panels show selected axons; arrows highlight regions of pGreen- or DsRed-positive axons where TRAK1 and TRAK2 expression can be compared between shRNA and scrRNA in transfected vs. nontransfected neurons. Images are representative of at least  $n = 20$  cortical neurons from at least  $n = 3$  independent transfections. Scale bars = 10  $\mu\text{m}$ .

labeling of transfected cells can be compared with that of neighbouring untransfected neurons (Fig. 3, right, for TRAK1 and TRAK2 in hippocampal neurons; Fig. 4,

right, for TRAK1 and TRAK2 in cortical neurons). shRNA knockdown of TRAK1 or TRAK2 had no apparent effect on TRAK1 and TRAK2 in cell bodies and

C  
O  
L  
O  
R



dendrites of both hippocampal (Fig. 3, left) and cortical (Fig. 4, left) neurons. However, when the axons of both hippocampal and cortical neurons were analyzed, there was a notable reduction in both TRAK1 and TRAK2 levels (Figs. 3, 4). In fact, TRAK1 and TRAK2 immunoreactivities were not detected in axons of neurons transfected with pDsRedTRAK1shRNA or pGreen-TRAK2shRNA, respectively. The discrepancy between knockdown in axons vs. cell bodies and dendrites may be due to high expression of endogenous TRAKs in these compartments. The levels of anti-TRAK1 and anti-TRAK2 immunoreactivities were similar when staining patterns with in-house and commercial anti-TRAK1 and anti-TRAK2 antibodies were compared (Figs. 3, 4).

### Comparison of the Axonal and Dendritic Distributions of TRAK1 and TRAK2 in Primary Neuronal Cultures

A recent article reported that, in hippocampal pyramidal neurons, TRAK1 is more prevalent in axons, whereas TRAK2 is more abundant in dendrites (van Spronsen et al., 2013). These researchers utilized in-house antibodies raised against fusion proteins that had significant amino acid sequence identity (Fig. 1). Although some characterization of these in-house antibodies was carried out, to corroborate the reported findings, the immunocytochemical distributions of TRAK1 and TRAK2 were carried out with our in-house and commercial antibodies in 7-DIV primary hippocampal and cortical neurons in conjunction with costaining with antibodies directed against the axonal marker tau and the dendritic marker MAP2.

F5 Figure 5 shows the distribution of endogenous TRAK1 and TRAK2 in conjunction with tau and MAP2 immunoreactivities in primary hippocampal (Fig. 5A) and cortical (Fig. 5B) neurons. To determine the localization of TRAK1 and TRAK2 in axons vs. dendrites, the fluorescence intensities were determined in the ImageJ plugin RGB\_Profiler. The highest intensity of >20 axons and >20 dendrites was measured and then normalized to the highest intensity of TRAK1 and TRAK2 in the cell bodies of the corresponding neurons. The normalized intensity of axons was compared with the normalized intensity of dendrites. For in-house and commercial antibodies in hippocampal neurons, it was observed that TRAK1 was expressed at approximately twice the level in dendrites. The values were TRAK1 in dendrites compared with axons  $0.49 \pm 0.12$  times (in-house antibodies, hippocampal neurons) and  $0.41 \pm 0.05$  times (commercial antibodies, hippocampal neurons). In cortical neurons, a similar pattern was observed for TRAK1 immunoreactivity; i.e., TRAK1 expression in dendrites was  $0.57 \pm 0.07$  times that in axons. However, with commercial anti-TRAK1 antibodies, an approximately equal distribution between axons and dendrites was observed. For TRAK2, a different distribution profile was seen. Thus, in hippocampal neurons for both in-house and commercial anti-TRAK2 antibodies, TRAK2 was highest in dendrites vs.

axons. Values were  $1.73 \pm 0.15$  times (in house) and  $1.54 \pm 0.10$  times (commercial) for dendritic vs. axonal distribution. In cortical neurons, there was an approximately equal distribution of TRAK2. This was the case for both commercial and in-house anti-TRAK2 antibodies.

### DISCUSSION

Because the brain is critically dependent on the supply of energy generated by mitochondria, understanding how they are trafficked to match requirements for function is important. The TRAK family of kinesin adaptor proteins are key mediators of mitochondrial transport. This study investigated the use of antibodies, both generated in-house and available commercially, to study the subcellular distribution of the two members of this gene family, TRAK1 and TRAK2, in two types of neurons in primary culture, i.e., hippocampal pyramidal and cortical neurons. A different distribution of TRAK1 and TRAK2 was evident between axons and dendrites and between the two neuronal types. In hippocampal neurons, both commercial and in-house antibodies yielded similar profiles, with TRAK1 being more abundant in axons compared with dendrites. By contrast, TRAK2 was expressed at higher levels in dendrites compared with axons. In neurons of cortical cultures, there was a discrepancy between commercial and in-house antibodies and also TRAK1 and TRAK2 subcellular compartmentalization. Whereas TRAK1 was enriched in axons but equally distributed between axons and dendrites with in-house antibodies, an equidistribution between axons and dendrites for both TRAK1 and TRAK2 was found for the localization with commercial antibodies. These empirical observations suggest that TRAK1 and TRAK2 do play distinct roles in the regulation of mitochondrial transport and hence, importantly, the delivery of a local supply of energy in the brain.

There has been only one article to date describing the subcellular distribution of TRAK1 and TRAK2 in one neuronal cell type, i.e., hippocampal pyramidal neurons at 14 DIV (van Spronsen et al., 2013). Although the findings reported here are generally in agreement for this neuronal type, i.e., for both in-house and commercial antibodies TRAK1 being more abundant in axons vs. dendrites and TRAK 2 vice versa, there are qualitative and quantitative differences between the two studies. For example, the percentage difference in distribution for endogenous TRAK2 vs. TRAK1 in dendrites is more marked in the van Spronsen et al. (2013) study; the immunolabeling in neuronal processes is more punctate than that described here (van Spronsen et al., 2013), and intense TRAK1 immunoreactivity was observed in the perinuclear region, which was less marked in the findings of van Spronsen et al. (2013). These differences may be attributed to developmental differences because in the current study immunolabeling was carried out at 7 DIV compared with 14 DIV by van Spronsen et al. (2013) or, alternatively, because of antibody specificity. It was

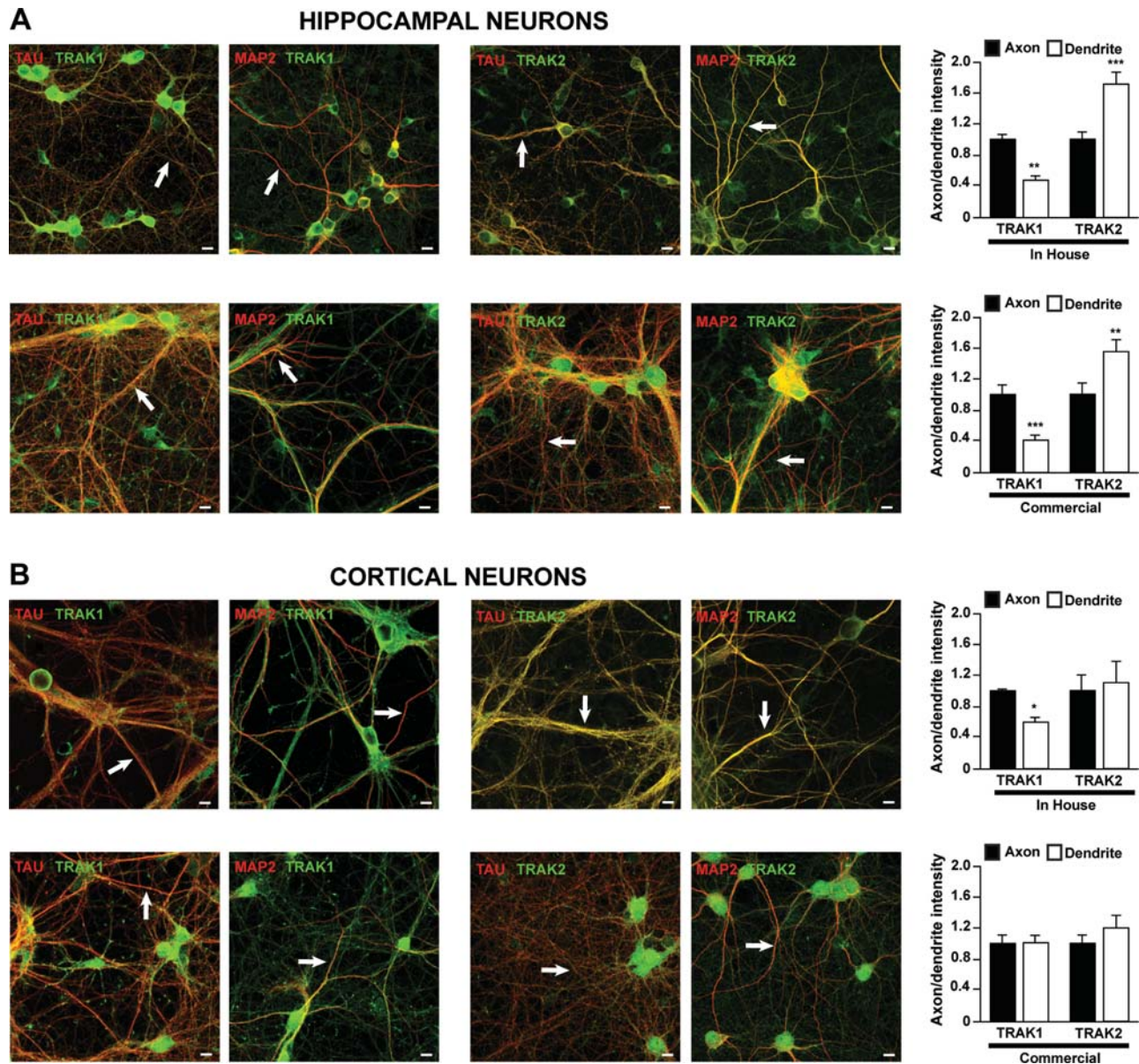


Fig. 5. Analysis of axonal and dendritic subcellular distribution of TRAK1 and TRAK2 in hippocampal pyramidal and cortical neurons with in-house and commercial anti-TRAK1 and anti-TRAK2 antibodies. Primary cultures of hippocampal pyramidal neurons (**A**) or cortical neurons (**B**) were costained with in-house (top) or commercial (bottom) anti-TRAK1 (green) or anti-TRAK2 (green) and either anti-tau (red) or anti-MAP2 (red) antibodies, with the distribution in axons vs. dendrites quantified as described in Materials and Methods. Arrows show representative examples for the codistribution of TRAK1 or TRAK2 with either tau or MAP2 immunoreactivities. The images are representative of at least  $n = 20$  neurons. Histograms

show the quantitative results. The highest fluorescent intensity in axons, normalized to the highest intensity of cell bodies, was set to a value of 1 and compared with the highest intensity in dendrites, also normalized against the highest intensity of cell bodies. Values for TRAK1 in dendrites compared with axons are  $0.49 \pm 0.12$  (in-house antibodies, hippocampal neurons) and  $0.57 \pm 0.07$  (in-house antibodies, cortical neurons). For TRAK2, values in dendrites compared with axons are  $1.73 \pm 0.15$  (in-house, hippocampal pyramidal neurons). Quantitative results were analyzed by Student's *t*-test, \* $P < 0.05$ , \*\* $P < 0.01$ , \*\*\* $P < 0.001$ . Scale bars = 10  $\mu\text{m}$ .

notable that, when hippocampal pyramidal neurons were treated with the TRAK1 shRNA, a reduction in TRAK1 immunolabeling was observed in processes but not in cell bodies (Fig. 4). This may be explained by high transcription of TRAK1 resulting in a decreased efficiency of

knockdown, the stability of TRAK1 in processes, or, alternatively, antibody specificity. The antibodies used in this study were characterized in depth using specific gene knockdown in conjunction with two experimental paradigms, immunoblotting and immunocytochemical

analyses. It was observed that, although the commercial antibodies recognized both TRAK1 and TRAK2 in immunoblots, they had profiles similar to those of the more selective in-house anti-TRAK1 and anti-TRAK2 antibodies with respect to distribution studies. There were, however, quantitative differences between commercial and in-house antibodies for axonal vs. dendritic localization. TRAKs are key components of a quaternary mitochondrial trafficking complex. Within this complex, motor proteins, Miro, and OGT all bind TRAKs at distinct sites, so there is always the potential for steric hindrance with regard to antibody binding. This is pertinent particularly for quantitative localization studies and supports the good practice of simultaneous use of antibodies with different specificities.

It is unclear why there should be a difference in TRAK1 distribution between axons and dendrites and, also, in TRAK2 distribution between hippocampal pyramidal and cortical neurons, where it was found to have an equal distribution between axons and dendrites. The observations vis-a-vis axonal vs. dendritic localization may be due in part to the availability of the motor proteins and the binding preferences of TRAK1 (kinesin preferring) and TRAK2 (dynein preferring) as proposed by van Spronsen et al., (2013). It may, alternatively, be a result of distinct developmental and overall expression levels of TRAK1 vs. TRAK2. Similarly, this may explain the differences between hippocampal vs. cortical neurons, or the distinct distributions might reflect the energy requirements of the different neuronal cell types. Further studies are required to establish the contribution of TRAK-mediated mitochondrial transport to its functional significance in meeting brain energy requirements.

## REFERENCES

- Attwell D, Laughlin SB. 2001. An energy budget for signaling in the grey matter of the brain. *J Cereb Blood Flow Metab* 21:1133–1145.
- Beck M, Brickley K, Wilkinson HL, Sharma S, Smith M, Chazot PL, Pollard S, Stephenson FA. 2002. Identification, molecular cloning, and characterization of a novel GABAA receptor-associated protein, GRIF-1. *J Biol Chem* 277:30079–30090.
- Brickley K, Stephenson FA. 2011. Trafficking kinesin protein (TRAK)-mediated transport of mitochondria in axons of hippocampal neurons. *J Biol Chem* 286:18079–18092.
- Brickley K, Smith MJ, Beck M, Stephenson FA. 2005. GRIF-1 and OIP106, members of a novel gene family of coiled-coil domain proteins: association in vivo and in vitro with kinesin. *J Biol Chem* 280:14723–14732.
- Brickley K, Pozo K, Stephenson FA. 2011. N-acetylglucosamine transferase is an integral component of a kinesin-directed mitochondrial trafficking complex. *Biochim Biophys Acta* 1813:269–281.
- Chan DC. 2006. Mitochondria: dynamic organelles in disease, aging, and development. *Cell* 125:1241–1252.
- Glater EE, Megeath LJ, Stowers RS, Schwarz TL. 2006. Axonal transport of mitochondria requires milton to recruit kinesin heavy chain and is light-chain independent. *J Cell Biol* 173:545–557.
- Goslin K, Asmussen H, Banker G. 1998. Rat hippocampal neurons in low-density culture. In: Banker G, Goslin K, editors. *Culturing nerve cells*. Cambridge, MA: MIT Press. p 339–370.
- Iyer SP, Akimoto Y, Hart GW. 2003. Identification and cloning of a novel family of coiled-coil domain proteins that interact with O-GlcNAc transferase. *J Biol Chem* 278:5399–5409.
- Kang JS, Tian JH, Pan PY, Zald P, Li C, Deng C, Sheng ZH. 2008. Docking of axonal mitochondria by syntaphilin controls their mobility and affects short-term facilitation. *Cell* 132:137–148.
- Kapitein LC, Schlager MA, Kuijpers M, Wulf PS, van Spronsen M, MacKintosh FC, Hoogenraad CC. 2010. Mixed microtubules steer dynein-driven cargo transport into dendrites. *Curr Biol* 20:290–299.
- Mattson MP, Gleichmann M, Cheng A. 2008. Mitochondria in neuroplasticity and neurological disorders. *Neuron* 60:748–766.
- Pekkmaz G, Trinidad JC, Wang X, Kong D, Schwarz TL. 2014. Glucose regulates mitochondrial motility via Milton modification by O-GlcNAc transferase. *Cell* 158:54–68.
- Peppiatt C, Attwell D. 2004. Neurobiology: feeding the brain. *Nature* 431:137–138.
- Pilling AD, Horiuchi D, Lively CM, Saxton WM. 2006. Kinesin-1 and dynein are the primary motors for fast transport of mitochondria in *Drosophila* motor axons. *Mol Biol Cell* 17:2057–2068.
- Schwarz TL. 2013. Mitochondrial trafficking in neurons. *Cold Spring Harbor Perspect Biol* doi: 10.1101/cshperspect.a011304.
- Stephenson FA, Brickley K. 2011. Mechanisms of neuronal mitochondrial transport. In: Wittenbach A, O'Connor V, editors. *Protein folding for the synapse*. Berlin: Springer. p 105–119.
- Stephenson FA, Duggan MJ. 1991. Molecular neurobiology: a practical approach. In: Chad J, Wheal H, editors. *Oxford: IRL Press*. p 183–204.
- van Spronsen M, Mikhaylova M, Lipka J, Schlager MA, van den Heuvel DJ, Kuijpers M, Wulf PS, Keijzer N, Demmers J, Kapitein LC, Jaarsma D, Gerritsen HC, Akhmanova A, Hoogenraad CC. 2013. TRAK/Milton motor-adaptor proteins steer mitochondrial trafficking to axons and dendrites. *Neuron* 77:485–502.
- Zheng Y, Wildonger J, Ye B, Zhang Y, Kita A, Younger SH, Zimmerman S, Jan LY, Jan YN. 2008. Dynein is required for polarized dendritic transport and uniform microtubule orientation in axons. *Nat Cell Biol* 10:1172–1180.

AQ1: Please confirm that given names (red) and surnames/family names (green) have been identified correctly.

WILEY  
Author Proof